Visualization of mobility by atomic force microscopy

Visualization of mobility by atomic force microscopy

Toshio Ando and Noriyuki Kodera

Running Head: Visualization by high-speed AFM

Summary

Intrinsically disordered regions (IDRs) of proteins are very thin and hence hard to be visualized by electron microscopy. Thus far, only high-speed atomic force microscopy (HS-AFM) can visualize them. The molecular movies identify the alignment of IDRs and ordered regions in an intrinsically disordered protein (IDP) and show undulation motion of the IDRs. The visualized tail-like structures contain the information of mechanical properties of the IDRs. Here, we describe methods of HS-AFM visualization of IDPs and methods of analyzing the obtained images to characterize IDRs.

Keywords: high-speed atomic force microscopy, AFM, high-speed AFM, visualization, dynamic imaging, mobility, mechanical properties

1. Introduction

There are several methods to analyze the structure of IDPs as described in this book. However, visualization of the IDRs is very difficult by conventional methods. As IDRs are very thin and highly mobile (and hence take a huge number of conformations), electron microscopy techniques are incapable of visualizing them *(1)*. IDPs are hardly crystallized and hence x-ray crystallography is ineffective for IDPs. AFM can visualize individual nanometer-scale objects under various environments *(2)*. However, its imaging rate is very low to capture highly mobile IDRs in aqueous solutions. Of course, the sample can be dried and immobilized on a substrate surface. However, the structures become thinner upon being dried, resulting in infeasibility of the visualization. Moreover, the drying process very likely alters the IDR structure, which should be avoided.

Thus far, visualization of IDRs immobilized on a substrate surface in aqueous solutions has not been successful, because chemical treatments of a substrate surface are apt to increase the surface roughness, which prevents discerning IDRs *(1)*. Thus, only HS-AFM can visualize IDRs that are weakly attached to a highly flat surface in buffer solutions, without chemical immobilization (Fig.1) *(1)*.

HS-AFM *(3, 4)* has already been applied to the observation of dynamic behavior of several proteins in action *(5-8)*, including the walking behavior of a motor protein myosin V along actin filaments *(5)* and the structural changes in bacteriorhodopsin in response to light illumination *(6)*. However, the dynamics of these proteins are much slower than that of IDRs on a substrate surface. To visualize highly mobile IDRs with very thin structures using HS-AFM, we need to consider several factors, which will be described in this chapter. The molecular movies of IDPs reveal several characteristics of IDPs including the location of the order and disordered regions in the molecules, mechanical properties of IDRs and dynamics of order-disorder transitions of IDRs. Methods to analyze the molecular movies will also be described.

2. Materials

2.1 Substrate Surface

Mica (natural muscovite or synthetic fluorophlogopite) has frequently been used as a substrate owing to its surface flatness at the atomic level over a large area *(9)*. It has a net negative charge and is therefore quite hydrophilic. For the following procedures, *see* Fig. 2.

1. Prepare mica disks (1–2 mm in diameter) from a mica sheet with thickness of < 0.1 mm by cutting holes using a sharp puncher (*see* **Note 1**).
2. Glue a mica disk to the top surface of a sample stage (a glass rod with 2mm diameter and 2 mm height) using epoxy and wait until it has dried (~1–2 h) (Fig. 2A).
3. Glue the sample stage onto the z-scanner of the HS-AFM apparatus using nail enamel, and leave it for 5–10 min (Fig. 2A) (*see* **Note 2**).
4. Press a Scotch tape to the surface of the mica disk and then smoothly remove the tape from the mica (Fig. 2B). The top layer of the mica will be removed with the tape, which can be checked by inspecting the surface of the removed tape.
5. Place a sample solution on the freshly cleaved mica disk surface for 1–3 min (Fig. 2C, D), and then rinse using an appropriate buffer solution and a piece of Kimwipe cleaning paper (Fig. 2E, F) (*see* **Note 3**).

2-2. Small cantilevers

Small cantilevers (BL-AC10DS-A2, Olympus: f_c in air 1.5 MHz, f_c in water 600 kHz, k_c ~0.1 N/m) are commercially available (Atomic Force F&E GmbH, Manheim, Germany). The small cantilevers with a sharp tip made by electron bean deposition (EBD) are also available as an option (this is highly recommended). Although not yet commercialized, small cantilevers will soon be available also from NanoWorld AG (Neuchâtel, Switzerland). When a scanning electron microscope (SEM; a low vacuum type is recommended) is available, sharp EBD tips can be easily made and the expensive small cantilever chips can be used repeatedly *(4)*.

1. Prepare a small container with small holes (~0.1 mm diameter) in the lid.
2. Put a piece of phenol crystal (sublimate) in the container.
3. Put the container in a SEM chamber (if available, under a low vacuum condition).
4. Put cantilevers on the lid of the container immediately above the small holes.
5. Wait for a while until mechanical drift ceases.
6. Irradiate a spot-mode electron beam onto the original tip of the cantilever. Under a low vacuum condition, the tip grows at a rate of ~1μm/min, while under a high vacuum condition it grows a few times slower (*see* **Note 4**).
7. Sharpen the tip (apex radius, ~25 nm) using a plasma etcher (*e.g.*, PE200E; South Bay Technology, California, USA) in argon or oxygen gas. The apex radius can be reduced to ~4 nm in the best case (*see* **Note 5**).

2-3. Buffer solutions

Prepare all solutions using pure water. Keep all solutions in glass bottles, not in plastic bottles. Pure water used for cleaning several instrument elements such as a cantilever holder, sample stage, etc. should also be kept in a glass bottle (*see* **Note 6, 7**). The composition of buffer solutions will be mentioned in Experimental Methods.

3. Experimental Methods

3-1. IDP Samples

1. Dilute a stock solution of an IDP (usually ~10 μM order) to 100–200 nM using an appropriate buffer solution containing protease inhibitors (*e.g.*, 1mM PMSF, 0.5 mM benzamidine, 20 μg/ ml TPCK).
2. Divide the diluted sample into small aliquots (~10 μl) and quickly freeze them us-

ing liquid nitrogen.

3. Just before AFM experiments, thaw an aliquot of the frozen sample and dilute it to 1–5 nM using an appropriate buffer solution containing protease inhibitors.
4. Store the further diluted sample on ice and use it within 6 h to avoid possible proteolysis.

Ordered domains in an IDP usually attach to a mica surface stably. However, when an IDP is comprised entirely of IDRs, its mobility on a mica surface is too fast to be imaged. In this case, the IDP with a small protein tag, such as GFP, chitin binding protein (CBP), glutathione-S-transferase (GST), or poly-His tag, has to be constructed. Introducing a small protein tag to either the N- or C-terminus of the IDP is recommended because it facilitates the identification of the termini of the imaged elongate molecule. The protein tags attach to a mica surface stably and thereby the mobility of IDRs is significantly reduced.

3-2. Buffer solutions

There is no unique choice for the buffer solution used for HS-AFM imaging. However, it is recommended to begin with using a low ionic strength solution such as (10 mM Tris-HCl, pH 7.5, 1 mM $MgCl_2$), because IDRs, which are often rich in both positively and negatively charged amino acids *(10)*, are only weakly adsorbed onto a bare mica surface. When the mobility of IDRs is too high to be imaged, the following changes are recommended for the buffer solution.

1. Change the concentration of divalent cations (Mg^{2+} or Ca^{2+}). Increase in the concentration facilitates binding of negatively charged amino acids of IDPs to a negatively charged mica surface.
2. Reduce the concentration of K^+ (if contained) which binds to a mica surface much more strongly than Na^+ and inhibits the electrostatic protein-surface interaction.
3. Change pH within an allowable range.

Once IDRs are imaged in a low ionic strength solution, the ionic strength should be increased gradually by increasing the concentration of NaCl to examine whether or not the structure of IDRs are influenced by the low ionic strength (*see* **Note 8, 9**).

3-3. HS-AFM imaging

The procedures for tapping-mode HS-AFM imaging, which will be described below, are basically the same as that for conventional tapping-mode AFM imaging. However, note that in the HS-AFM apparatus (Fig. 3), the cantilever and the sample are arranged upside-down, so that the cantilever tip points upward to the sample (Fig. 2G) *(3, 4)*. The HS-AFM apparatus will be commercially available worldwide in 2011 from Research Institute of Biomolecule Metrology, Co. Ltd., Tsukuba, Japan)

1. Place a buffer solution (~60 μl) around the cantilever installed in its holder of the HS-AFM apparatus (*see* **Note 10**).
2. Install the scanner, which has a sample on the z-scanner through the mica-attached sample stage, in the HS-AFM apparatus so that the sample is immersed in the buffer solution placed around the cantilever (Fig. 2G).
3. Adjust the positions of the cantilever and the sample stage by observing them through an objective lens of the optical beam deflection (OBD) detector, optical components, a CCD camera, and a video display that are implemented in the HS-AFM apparatus.
4. Adjust the position of the incident laser beam from the OBD detector so that it is focused onto the cantilever.
5. Find the cantilever resonant frequency by measuring the power spectrum of thermal fluctuations in the cantilever deflection.
6. Excite the cantilever by applying AC voltage to a piezoactuator attached to the cantilever holder. Adjust the frequency of the AC voltage at the resonant frequency of the cantilever.
7. Finely adjust the laser beam position so that the maximum amplitude signal from the OBD detector appears (thus, the optimum sensitivity is attained) (*see* **Note 11**).
8. Start tip-sample approach by driving a stepper motor attached to the scanner.
9. Once the cantilever tip makes contact with the sample, slightly move the sample stage upward to break the tip-sample contact by changing the off-set DC voltage for the z-scanner and then measure an amplitude-distance curve to estimate the sensitivity of the amplitude signal to the tip-sample interaction.
10. Slightly move the sample stage upward to break the tip-sample contact again and then readjust the AC voltage for cantilever excitation to attain appropriate free oscillation amplitude of the cantilever (A_0).
11. Adjust the amplitude set point (A_s) at ~$0.95 \times A_0$.
12. Set the values of parameters for the scan size, number of scan lines, and scan speed.

13. Switch on the proportional-integral-derivative (PID) feedback circuit (*see* **Note 12**).
14. Start imaging (Fig. 2H).
15. Readjust the amplitude set point so that clear images are obtained (*see* **Note 12**).
16. Move the imaging area by changing the off-set DC voltages for the x- and y-scanners. By repeating this operation and video imaging, we can quickly find IDP molecules and record dynamic behaviour of many IDP molecules.

In HS-AFM, the alteration of imaging parameters is quickly reflected in the images. Therefore, the operation of HS-AFM is easier than conventional AFM. However, we have to take the following considerations into account to successfully visualize IDRs.

1. Cantilever oscillation amplitude: To minimize the tip-sample interaction force, A_0 and A_s should be adjusted to ~1 nm and 0.9–0.95 × A_0, respectively.
2. Scan range: Within a scan range of 100 × 100 nm^2, the entire of one or two IDP molecules appears when a 1–5 nM sample is applied to a mica surface. This scan size or a slightly smaller size is appropriate for high-speed imaging of IDRs.
3. Imaging rate: Mobile IDRs are usually captured on video at an imaging rate of 10–15 fps. When a higher imaging rate is necessary to record highly undulating IDRs, the imaging rate can be increased only by reducing the scan range and the number scan lines. Although a higher rate of imaging with a wider imaging area is possible, the resulting insufficient feedback operation will damage or fillip the IDP molecules due to too strong tip-sample interaction.

4. Image Analysis

4-1. Determination of N- and C-termini

When an IDP is comprised of ordered and disordered regions, we first estimate which end of the imaged elongate molecule is the N-terminus by comparing the image with theoretical predictions for the ordered and disordered regions of the protein (an example is shown in Fig.1). We can thereby estimate the locations of these regions in terms of the amino acid sequence. However, this estimation sometimes needs to be checked by the below-mentioned additional experiments when the arrangement of the ordered and disordered regions of imaged molecules differs from that provided by the theoretical predictions (*see* **Note 13**). When the arrangement is roughly symmetric along the elongated molecule, we also need to conduct the additional experiments.

1. Take images of partially proteolyzed samples of the IDP when the proteolysis products are already characterized (*see* **Note 14**).
2. Take images of an IDP construct with a small protein tag at either the N- or C-terminus.

4-2. Height and width of IDR

AFM images can provide the information of sample height with sub-nanometer accuracy. The identification of IDRs can be made by measuring the sample height.

1. Take cross-section profiles of the imaged tail-like structure at various positions along the structure.
2. Subtract the average height of portions at sample-free substrate surface from the peak heights of the cross-section profiles.
3. Make a histogram of the subtracted peak heights.

The histogram usually shows a Gaussian distribution, and therefore, the height value corresponding to the peak of the distribution is considered as the height of the IDR. The height of IDRs is 0.4–0.5 nm, which can be used as a criterion for judging the imaged tail-like structure to be an IDR (*see* **Note 15**). The width ($2w$) of an imaged IDR is largely affected by the tip radius R: $w = (R\rho)^{1/2}$, where ρ is the radius of an IDR. When R is inspected by electron micrographs of the tip, the value of ρ can be estimated using the equation $w = (R\rho)^{1/2}$. However, the mobility of IDRs is often very high, so that they move during capturing one image. In this case, the width is only roughly estimated.

4-3. Mechanical properties of IDR

The tail-like structure of an IDR can be viewed as a macroscopic or microscopic one (Fig. 4) *(1)*. An AFM image of an IDR only provides its macroscopic view because the spatial resolution of AFM is insufficient to resolve the polypeptide chain. The stiffness of a macroscopically viewed IDR string is described by the persistence length p of the string. In two dimensions, the mean square point-to-point distance of the string is given by

$$< r^2(l) >_{2D} = 4pl\left[1 - \frac{2p}{l}\left(1 - e^{-l/2p}\right)\right], \qquad (1)$$

where l is the contour length between two points on the string *(11)*. We can estimate the value of p from the result of best fitting of eq. (1) to the plot $<r^2(l)>_{2D}$ *vs.* l (Fig.

4c). The value of p is usually 11-12 nm for IDPs *(1)* (*see* **Note 16**) and thus can be used as a criterion for judging the imaged tail-like structure to be an IDR.

When the one-to-one correspondence is cleared between the imaged IDR and its amino acid sequence, we can estimate the microscopic persistence length L_p of the IDR. L_p does not represent the stiffness but represents how loosely the polypeptide chain is folded; when L_p is small, its polypeptide chain is well folded. For an ordered globular protein, L_p is known to be 0.3–0.5 nm *(13, 14)*. The microscopic contour length L_c (*i.e.*, polypeptide chain length) is larger than the macroscopic contour length. Therefore, for the relationship between the end-to-end distance of the IDR ($L_{E\text{-}E}$) and L_c, we can approximately use an equation $\langle L_{E\text{-}E}^2 \rangle = 4L_pL_c$ which is obtained from eq. (1) for $l \rightarrow \infty$. L_c can be estimated by $N_{aa} \times 0.34$ nm, where N_{aa} represents the number of amino acids contained in the IDR and '0.34 nm' is the average distance between the nearest neighbour amino acids. When either end of an IDR adjoins an ordered region, we first measure the direct distance between the free end of the IDR and the center of the ordered region and then subtract the half of the height value of the ordered region from the measured distance to estimate the $L_{E\text{-}E}$. When an IDR locates between two ordered regions, we first measure the direct distance between the centers of the ordered regions and then subtract half of the sum of the height values of the ordered regions to estimate the $L_{E\text{-}E}$. Interestingly, the value of L_p is usually in a small range of 1.2–1.3 nm for IDRs *(1)* (*see* **Note 16**). Therefore, this is also used as a criterion for judging the imaged tail-like structure to be an IDR.

4-4. Order-disorder transition

An IDR is not necessarily always in disordered conformations. Some IDRs show reversible transitions between the ordered and disordered states, which clearly appear in the AFM images; the ordered conformation gives a bright image while the disordered conformation gives a dark image. By measuring the average lifetimes of the ordered state ($\langle \tau_O \rangle$) and the disordered state ($\langle \tau_D \rangle$), we can estimate the free energy difference ($\Delta E = E_O - E_D$) between the two states using the equation *(15)*

$$\frac{\tau_O}{\tau_D} = exp\left(-\Delta E / k_B T\right) \qquad (2).$$

5. Notes

1. Serrated edge formation, which often accompanies partial cleavage of interlayer contacts in the mica disk, should be avoided. Hydrodynamic pressure produced by rapid scanning of the sample stage induces vibrations of the disk through movement of the cleaved sites. For high-speed imaging, the disk should be small (1-2 mm in diameter) to avoid generation of too large a hydrodynamic pressure *(16)*.
2. The sample stage should be removed from the z-scanner soon after performing experiments, using ethanol or acetone. When the stage is tightly glued to the z-scanner after letting it stand for a long time, the removal becomes difficult and its forced removal often breaks the z-scanner.
3. Do not tear a cleaning paper to pieces. Avoid the cleaning paper being touched with the mica surface. The cleaning paper should be touched briefly with a sample solution on the surface. Otherwise, dust particles will be contaminated
4. The total tip length (original tip + EBD tip) should be longer than 2.5 μm. Otherwise, a so-called “squeeze effect” becomes significant. When an oscillating cantilever is close to the substrate surface, the solution sandwiched between them is squeezed, which damps the cantilever oscillation and lowers the quality of AFM images.
5. The plasma etcher also can be used for cleaning used cantilevers, which lengthens the lifetime of expensive small cantilevers.
6. When water or buffer solutions are kept in plastic bottles for a long time, nanoparticles ooze out into the solutions.
7. The cantilevers, cantilever holder and sample stage should be cleaned after performing AFM experiments and stored in a clean container.
8. Since not many IDPs are thus far imaged by HS-AFM, the identification of the ordered and disordered regions by AFM may be claimed to be artefacts due to the surface-sample interaction or the low ionic solutions used. To remove the possible artefact arising from the use of a low ionic solution, it is best to use a higher ionic solution if it does not increase the mobility too much.
9. For a limited numbers of IDPs examined thus far by HS-AFM, we have not found discrepancy between the AFM and NMR results in the identification of the ordered and disordered regions of the IDPs.
10. In HS-AFM, the z-piezoactuater is installed close to the sample stage immersed in a solution. When the volume of buffer solution exceeds a certain level, the solution touches the z-piezoactuator, leading to irreparable damage of the z-piezoactuator.
11. Because the cantilevers for high-speed imaging are very small, precisely aligning

the laser beam position relative to a small cantilever cannot be made by the optical view through a ×20 objective lens installed in the OBD detector. Therefore, the best alignment is judged by the optimum sensitivity of the OBD detection.

12. When the amplitude set point A_s is larger than $0.95 \times A_0$, the tip often completely detaches at steep downhill regions of the sample (parachuting). During parachuting, bright streaks leaving long tails in the x-direction appear. By gradually getting A_s smaller, these bright streaks disappear and clear images are obtained. However, avoid setting A_s smaller than $0.9 \times A_0$ even when clear images appear. Otherwise, the sample will be damaged. The PID controller implemented in the HS-AFM apparatus is specially designed so that parachuting does not occur as far as A_s is smaller than ~$0.9–0.95 \times A_0$ *(4, 17)*.
13. When predicted ordered and disordered regions have relatively small number of amino acids, the accuracy of the prediction seems low. We have to consider the prediction only as a reference.
14. Analysis of proteolysis products of IDPs has often been carried out to identify the locations of the ordered and disordered regions in the amino acid sequence, particularly in NMR analysis of IDPs. However, we have to keep it in mind that even partial proteolysis possibly removes segments critical for forming disordered or ordered regions.
15. A tail-like flexible structure of an imaged molecule does not necessarily means that it is an IDR.
16. This statement is made based on HS-AFM imaging of a few numbers of IDPs. Therefore, we are not yet sure whether this is the case for any IDRs. However, if this is the case, it means that there is no stable state with an intermediate level of disorder (or order) and the intermediate level of disorder may only appear temporarily during transitioning between the highly ordered and completely disordered structure. This issue remains an open question.

Acknowledgement

This work was supported by Grant-in-Aid for Basic Research (S) from JSPS, Knowledge Cluster/MEXT–Japan, and Grant-in Aid for Scientific Research on Innovative Areas (Research in a Proposed Research Area)/MEXT–Japan.

References

1. Miyagi A, Tsunaka Y, Uchihashi T, Mayanagi K et al (2008) Visualization of intrinsically disordered regions of proteins by high-speed atomic force microscopy. Chem Phys Chem 9:1859–1866.
2. Binnig G, Quate CF, Gerber Ch. (1986) Atomic force microscopy. Phys Rev Lett 56:930–933.
3. Ando T, Kodera N, Takai E et al (2001) A high-speed atomic force microscope for studying biological macromolecules. Proc. Natl Acad Sci USA 98:12468–12472.
4. Ando T, Uchihashi T, Fukuma T (2008) High-speed atomic force microscopy for nanivisualization of dynamic biomolecular processes. Prog Surf Sci 83:337–437.
5. Kodera N, Yamamoto D, Ishikawa R, Ando T (2010) Video imaging of walking myosin V by high-speed atomic force microscopy. Nature 468:72–76.
6. Shibata M, Yamashita H, Uchihashi T et al (2010) High-speed atomic force microscopy shows dynamic molecular processes in photo-activated bacteriorhodopsin. Nat Nanotechnol 5:208–212.
7. Yamamoto D, Uchihashi T, Kodera N, Ando T (2008) Anisotropic diffusion of point defects in two-dimensional crystal of streptavidin observed by high-speed atomic force microscopy. Nanotechnology 19:384009 (9 pp).
8. Milhiet P-E, Yamamoto D, Berthoumieu O et al (2010) Deciphering the structure, growth and assembly of amyloid-like fibrils using high-speed atomic force microscopy. PLos One 5:e13240 (8 pp).
9. Yamamoto D, Uchihashi T, Kodera N et al (2010) High-speed atomic force microscopy techniques for observing dynamic biomolecular processes. Methods Enzymol 475 (B):541–564.
10. Uversky VN, Dunker AK (2010) Review Understanding protein non-folding. Biochim Biophys Acta 1804:1231–1264.
11. Strobl G.R. (1996) The physics of polymers, Springer-Verlag, Berlin.
12. Manning GS (2006) The persistence length of DNA is reached from the persistence length of its null isomer through an internal electrostatic stretching force. Biophys J 91:3607–3616.
13. Dietz H, Rief M (2004) Exploring the energy landscape of GFP by single-molecule mechanical experiments. Proc Natl Acad Sci USA 101:16192–16197.
14. Müller DJ, Baumeister W, Engel A (1999) Controlled unzipping of a bacterial surface layer with atomic force microscopy. Proc Natl Acad Sci USA 96:13170–13174.
15. Yamashita H, Voïtchovsky K, Uchihashi T et al (2009) Dynamics of bacteriorhodopsin 2D crystal observed by high-speed atomic force microscopy. J Struct Biol 167:153–158.
16. Ando T, Kodera N, Maruyama D et al (2002) A High-speed atomic force microscope for studying biological macromolecules in action. Jpn J Appl Phys 41:4851–4856.

17. Kodera N, Sakashita M, Ando T (2006) Dynamic proportional-integral-differential controller for high-speed atomic force microscopy. Rev Sci Instrum 77:083704 (7 pp).
18. Romero P, Obradovic Z, Kissinger CR et al (1997) Identifying disordered proteins from amino acid sequences. Proc IEEE Int Conf Neural Networks 1:90–95.

Figure Captions

Figure 1: Prediction by PONDR (Predictor Of Naturally Disordered Regions, http://www.pondr.com/) *(18)* for the ordered and disordered regions of an IDP (a) and AFM images of the IDP weakly attached to a mica surface in a low ionic strength solution (b). Imaging rate, 23.8 fps (42 ms/frame); scan range, 80 × 80 nm^2; scale bar 20 nm. The number in each image represents the time stamp.

Figure 2: Sample preparation procedures for HS-AFM imaging. For details, see the text.

Figure 3: Schematic of HS-AFM apparatus.

Figure 4: Schematic of macroscopic (a) and microscopic (b) views of an IDR and a plot of the mean-square point-to-point distance as a function of the macroscopic contour length of an imaged IDR *(1)*. The solid line represents the best-fit curve of eq. (1).

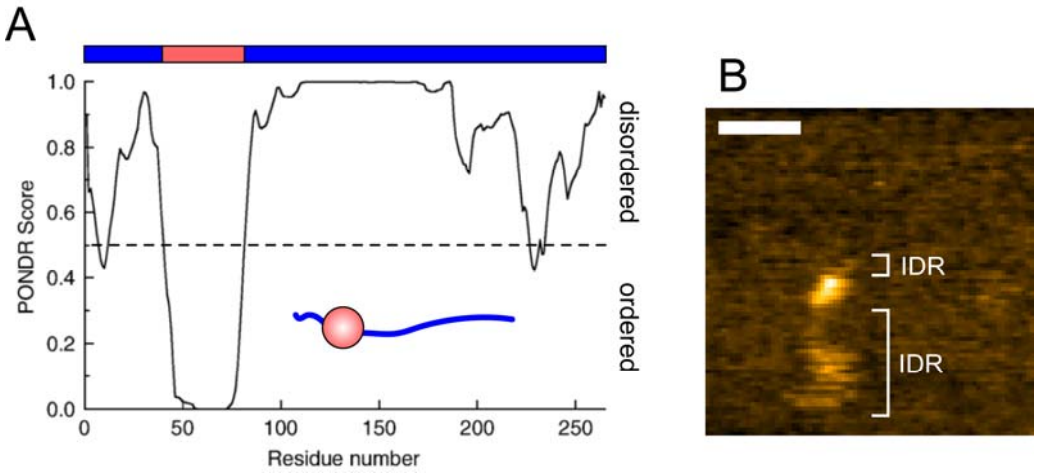
A
1.0
0.8
0.6
0.4
0.2
0.0
PONDR Score
0
50
100
150
200
250
Residue number
disordered
ordered
B
IDR
IDR

Figure 1

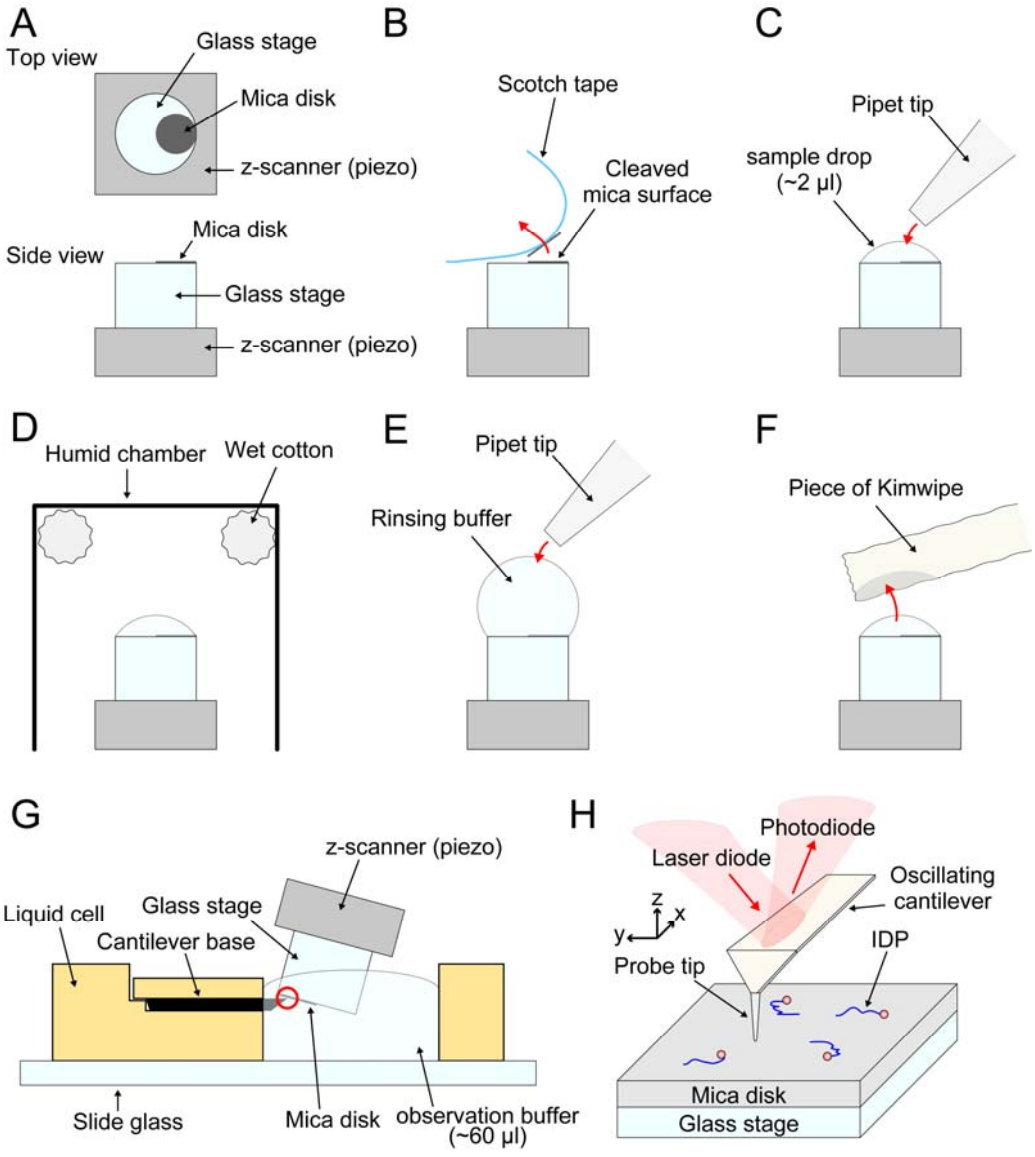
A
Top view
Glass stage
Mica disk
z-scanner (piezo)
Side view
Mica disk
Glass stage
z-scanner (piezo)
B
Scotch tape
Cleaved
mica surface
C
Pipet tip
sample drop
(~2 µl)
D
Humid chamber
Wet cotton
E
Pipet tip
Rinsing buffer
F
Piece of Kimwipe
G
z-scanner (piezo)
Liquid cell
Glass stage
Cantilever base
Slide glass
Mica disk
observation buffer
(~60 µl)
H
Photodiode
Laser diode
Oscillating
cantilever
z
x
y
IDP
Probe tip
Mica disk
Glass stage

Figure 2

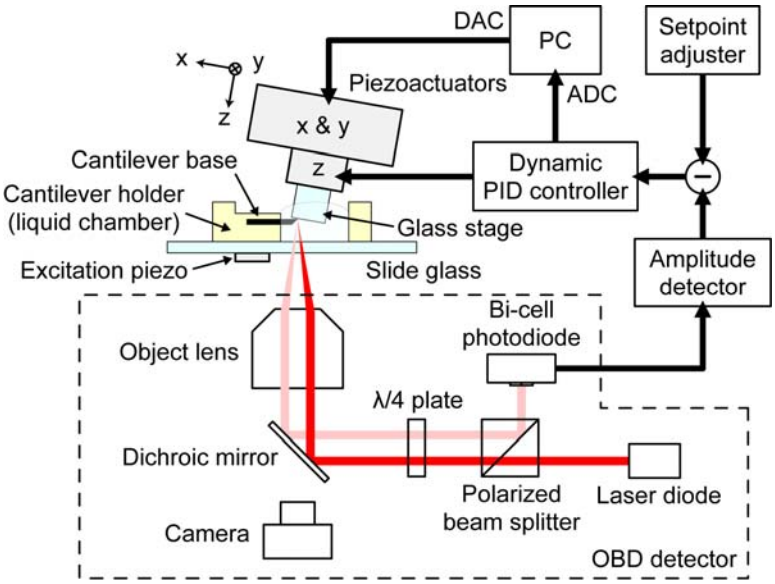
DAC
PC
Setpoint adjuster
x
y
z
Piezoactuators
ADC
x & y
z
Cantilever base
Cantilever holder (liquid chamber)
Dynamic PID controller
Glass stage
Excitation piezo
Slide glass
Amplitude detector
Bi-cell photodiode
Object lens
λ/4 plate
Dichroic mirror
Polarized beam splitter
Laser diode
Camera
OBD detector

Figure 3

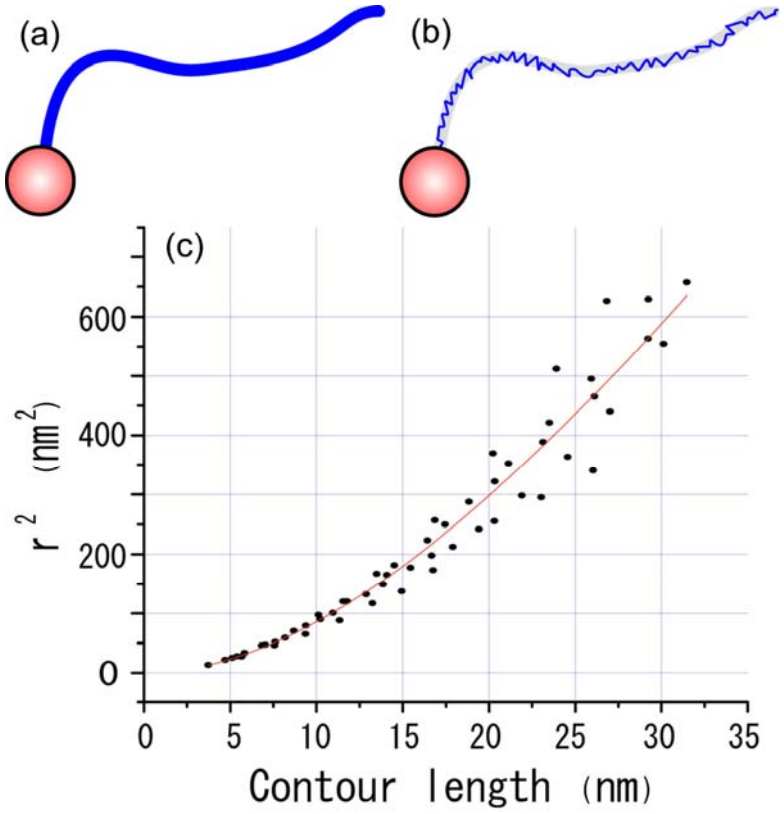

Figure 4